nature materials

SUPPLEMENTARY INFORMATION

DOI: 10.1038/NMAT4489

Hydrogels with tunable stress relaxation regulate stem cell fate and activity

Ovijit Chaudhuri[1–3†], Luo Gu[1,2†], Darinka Klumpers[1,2,4], Max Darnell[1,2], Sidi A. Bencherif [1,2], James C. Weaver[2], Nathaniel Huebsch[1,5], Hong-pyo Lee[3], Evi Lippens[2,6], Georg N. Duda [6], and David J. Mooney[1,2*]

[1]School of Engineering and Applied Sciences, Harvard University, Cambridge, MA 02138, USA.

[2]Wyss Institute for Biologically Inspired Engineering, Harvard University, Cambridge MA 02138, USA.

[3]Department of Mechanical Engineering, Stanford University, Stanford, CA 94305, USA

[4]Dept. Orthopedic Surgery, Research Institute MOVE, VU University Medical Center, Amsterdam, The Netherlands

[5]Gladstone Institute of Cardiovascular Disease, San Francisco

[6]Julius Wolff Institute, Charité – Universitätsmedizin Berlin and Berlin-Brandenburg Center for Regenerative Therapies, Berlin

†These authors contributed equally to this work.

*Correspondence to: mooneyd@seas.harvard.edu

SUPPLEMENTARY INFORMATION

Supplementary Note 1 – Range of strains and stresses relevant to cell-ECM interactions and tissues

An important question that arises from these studies is: what are the stresses and strains relevant to cell-ECM interactions and tissues? With relation to the relevance for cell-ECM interactions, various different strains have been reported. In 2D culture of cells on acrylamide gels, strains of 3 – 4% have been typically observed[1]. However, in 3D culture of fibroblasts in PEG gels, strains of 20 – 30% are typically observed, with strains as high as 50% measured immediately adjacent to cellular protrusions[2]. Therefore, the strain of 15% that is applied to hydrogels for the stress relaxation tests appears to be within the range of strains generated by cells. With relation to tissues, many tissues likely exhibit significant strains on the order of or exceeding 15% during activities such as breathing, muscle contraction, daily movement, skin stretching. Measurements have reported strains of 5 – 15% for alveoli in the lung during breathing[3], ~30% for muscles during contraction[4], and up to ~40% on skin of the knee during movement[5].

As a further point of comparison, the peak stresses measured during the stress relaxation tests can be compared with the range of stresses cells are capable of generating. Cells on 2D acrylamide gels[6] or encapsulated within 3D collagen[7] or PEG gels[2] generate traction stresses on the order of 100 to >1,000 Pa. Peak stresses measured during our stress relaxation tests are: ~310 Pa for brain, ~380 Pa for liver, ~150 Pa for fat, ~70 Pa for coagulated marrow, and ~1 kPa for a fracture hematoma (Supplementary Table 1). All values lie within the range of stresses cells are capable of generating.

Together, these highlight that the stress relaxation tests are probing a range of stress and strain relevant to cell-ECM interactions.

Supplementary Note 2 – Fitting the stress relaxation data to a linear viscoelastic model

The stress relaxation data of the alginate gels were analyzed in order to determine whether the alginate gels could be modeled as linear viscoelastic materials. Stress relaxation behaviors of some simple viscoelastic materials can be modeled with Maxwell model[8], in which the material is modeled as a spring and a dashpot in series (Supplementary Figure S1). With this model, the stress relaxation behavior should take the form of:

$$\sigma = \sigma_0 e^{-t/\tau_0} \quad (1)$$

This behavior represents a material with a single characteristic timescale for relaxation, typically corresponding to a specific molecular relaxation event that gives the material is viscosity. More complex linear viscoelastic materials may have multiple molecular mechanisms underlying their stress relaxation behavior, or exhibit a distribution of timescales for a single molecular relaxation event. These materials can sometimes be modeled with the Maxwell-Weichert model, consisting of multiple Maxwell models in parallel (Supplementary Figure S1). The stress relaxation behavior for a Maxwell model with *n* elements in parallel is:

$$\sigma = \sum_n \sigma_n e^{-t/\tau_n} \quad (2)$$

The stress relaxation data for the different alginate gels with an initial elastic modulus of 9 kPa were fit to simple Maxwell models and Maxwell-Weichert models with 2 Maxwell elements in parallel (Supplementary Figure S1). Good fits were obtained for the 2-element models, and the best-fit parameters are shown in Supplementary Table 3. It is possible that the different timescales represent specific molecular events, such as single calcium crosslink unbinding, G-block release when all calcium

crosslinks linking the G-block unbind, or the release of polymer entanglements. Alternatively, the requirement for two characteristic timescales for a good fit may result from a distribution of polymer length, G-block lengths, and G-block occupancy in the alginate gels.

Additional references:

1. Discher, D. E., Janmey, P. & Wang, Y.-L. Tissue cells feel and respond to the stiffness of their substrate. *Science* **310,** 1139–1143 (2005).
2. Legant, W. R. *et al.* Measurement of mechanical tractions exerted by cells in three-dimensional matrices. *Nat Meth* **7,** 969–971 (2010).
3. Huh, D. *et al.* Reconstituting organ-level lung functions on a chip. *Science* **328,** 1662–1668 (2010).
4. Gordon, A. M., Huxley, A. F. & Julian, F. J. The variation in isometric tension with sarcomere length in vertebrate muscle fibres. *J. Physiol.* **184,** 170–192 (1966).
5. Wessendorf, A. M. & Newman, D. J. Dynamic understanding of human-skin movement and strain-field analysis. *IEEE Trans. Biomed. Eng.* **59,** 3432–3438 (2012).
6. Lo, C. M., Wang, H. B., Dembo, M. & Wang, Y. L. Cell movement is guided by the rigidity of the substrate. *Biophys. J.* **79,** 144–152 (2000).
7. Legant, W. R. *et al.* Microfabricated tissue gauges to measure and manipulate forces from 3D microtissues. *Proc. Natl. Acad. Sci. U. S. A.* **106,** 10097–10102 (2009).
8. Findley, W. N., Lai, J. S. & Onaran, Kasif. *Creep and Relaxation of Nonlinear Viscoelastic Materials*. (1989).

Supplementary Figures and Legends

Supplementary Figure S1

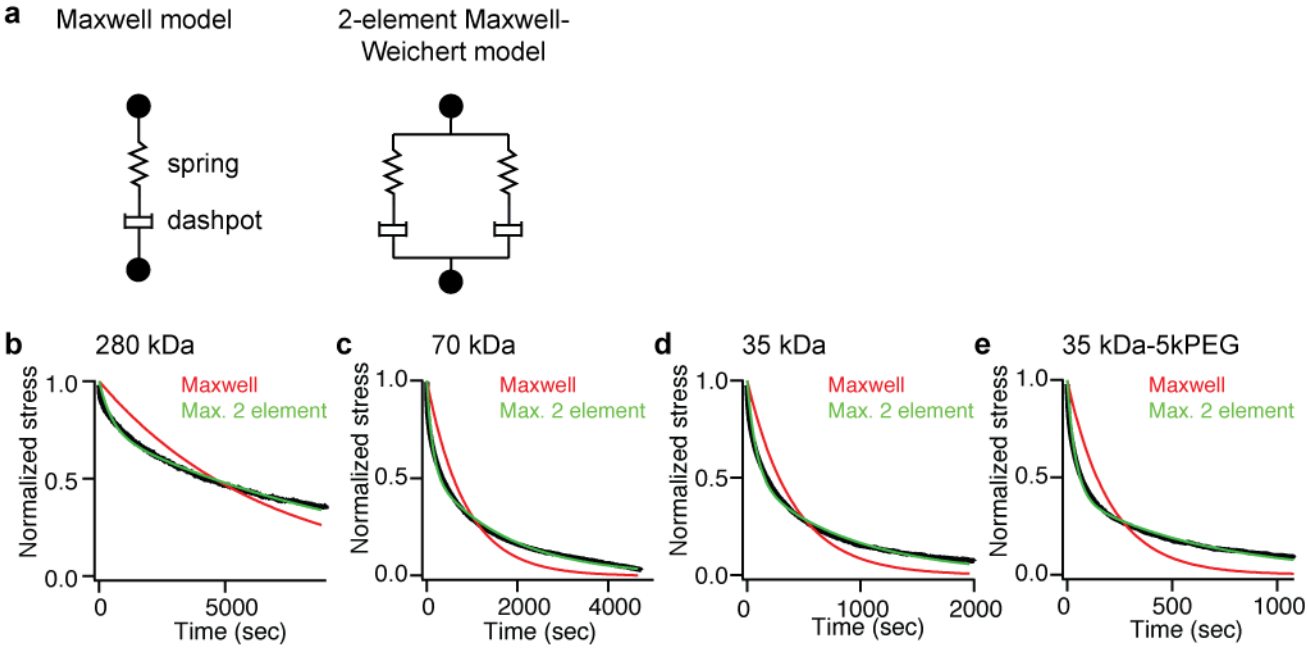

Supplementary Figure S1| Fitting of stress relaxation data to linear viscoelastic models. a, Schematic of two different linear viscoelastic models. **b,** Fit of stress relaxation data (black) to the linear viscoelastic models (red, green) for each hydrogel formulation. Molecular weight listed in each graph corresponds to the type of alginate used.

Supplementary Figure S2

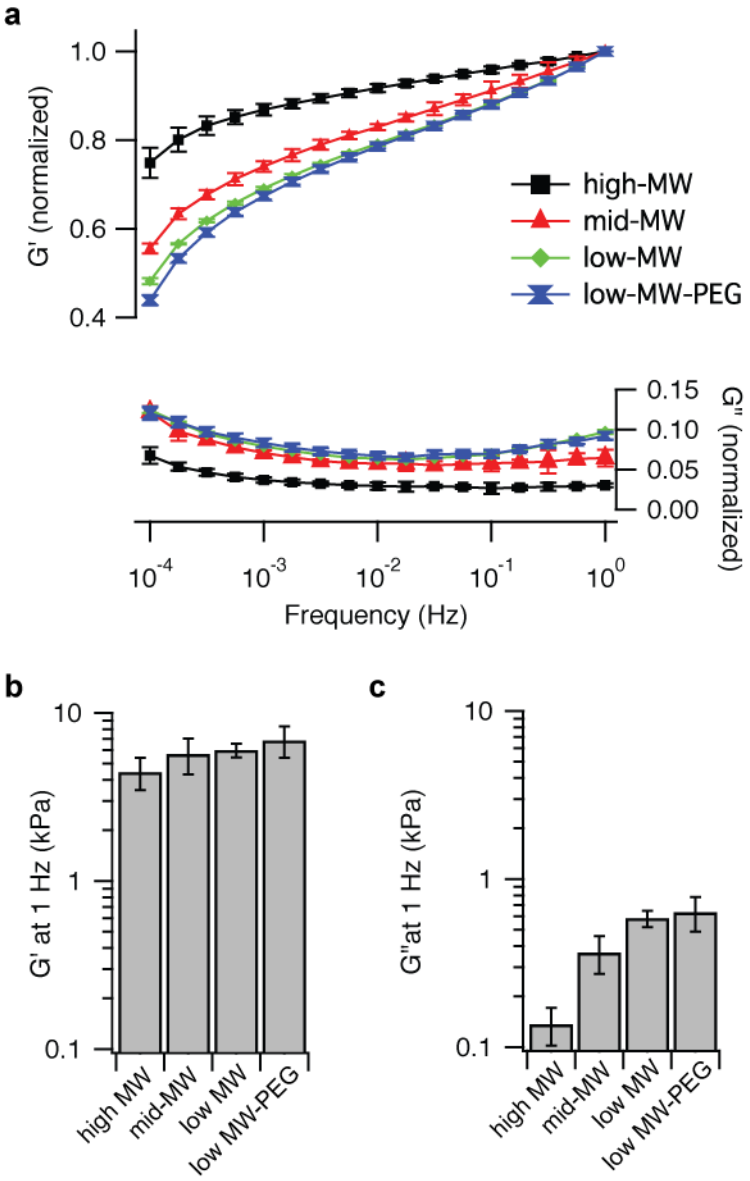

Supplementary Figure S2| Rheology of alginate hydrogels. a, Frequency sweep of shear storage and shear loss modulus of alginate hydrogels composed of the indicated alginate. Measurements conducted at 1% strain and all values are normalized by G' for the specific gel at 1 Hz. **b,** shear storage modulus at 1 Hz. **c,** shear loss modulus at 1 Hz. Note that in rheology experiments, gels are formed directly in rheometer and are not equilibrated in cell culture media. Therefore, these values cannot be directly compared with compression testing results, since gels are equilibrated in media before compression

testing and during cell culture experiments. Data are shown as mean +/- s.d, but s.d. is too small to be visible for most data points in **a**.

Supplementary Figure S3

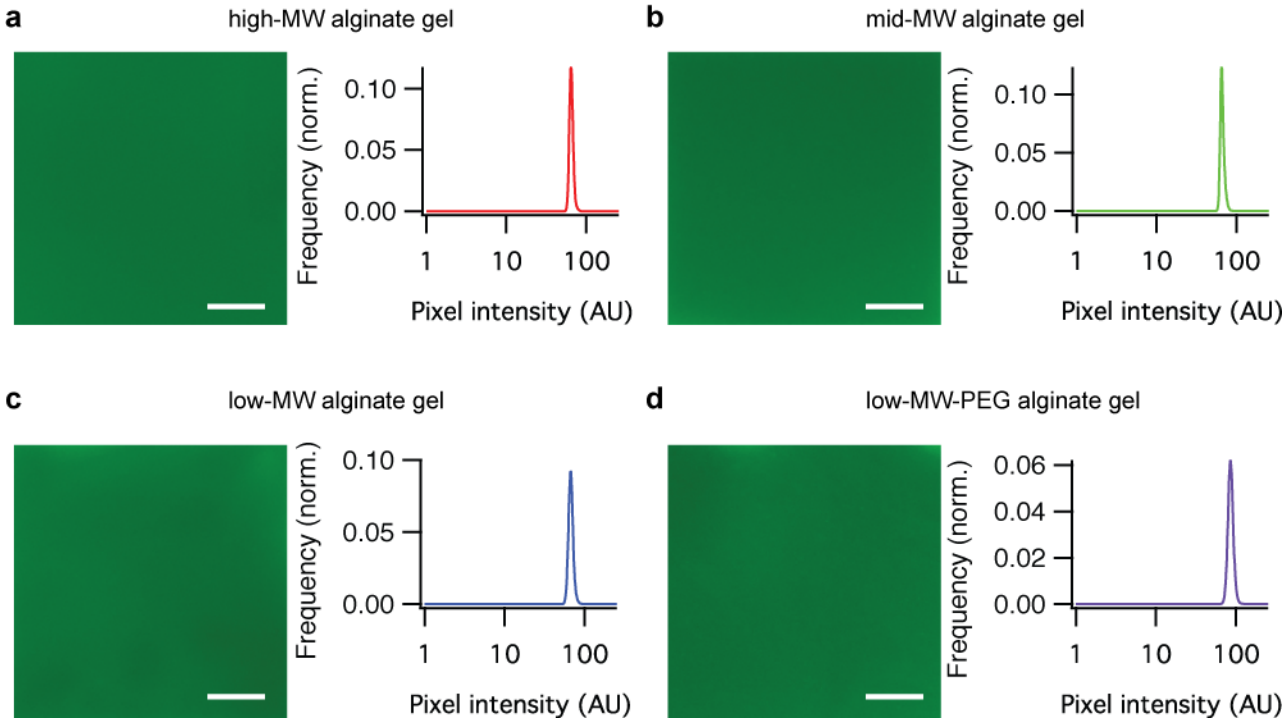

Supplementary Figure S3| Homogeneity of alginate gels at the microscale. a – d, Representative confocal fluorescence images of the different formulations of alginate gels are shown on the left of each sub-figure. On the right of each sub-figure are averaged normalized histograms of pixel intensities determined from multiple images taken from at least 3 gels. Scale bar is 50 μm.

Supplementary Figure S4

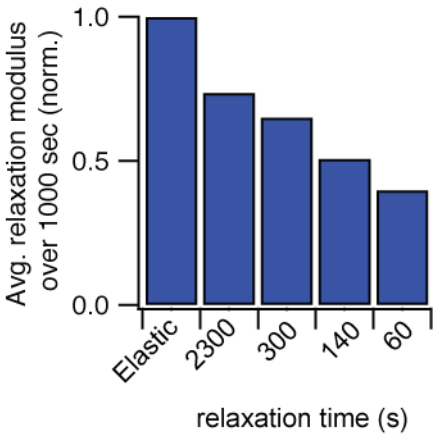

Supplementary Figure S4| Average value for the relaxation modulus over the first 1000s of a stress relaxation test normalized by the initial elastic modulus. Elastic column represents the expectation for an ideal elastic gel and is not based on an actual stress relaxation test.

Supplementary Figure S5

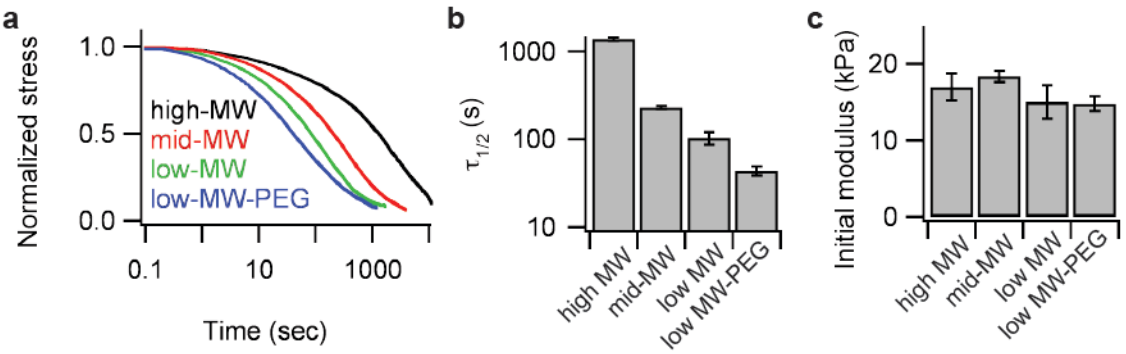

Supplementary Figure S5| Mechanical characterization of alginate hydrogels with an initial modulus of 17 kPa. a, Stress relaxation tests of alginate hydrogels with an initial modulus of ~17 kPa with a compressional strain of 15%. **b**, $\tau_{1/2}$ for gels in **a**. Timescale of stress relaxation decreases significantly with alteration in architecture (Spearman's rank correlation coefficient, $p < 0.0001$). **c,** Initial modulus of the gels in **a.** No significant dependence between initial modulus and matrix architecture is measured, as judged by spearman's rank correlation test.

Supplementary Figure S6

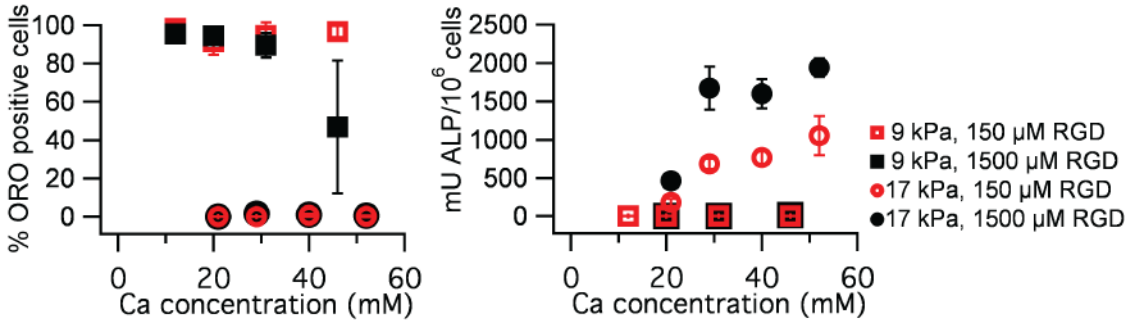

Supplementary Figure S6| MSC differentiation not correlated with calcium crosslinking concentration in this study. Quantification of percentage of cells that stain positive for ORO and alkaline phosphatase activity for D1 cells encapsulated in the indicated conditions as a function of the concentration of calcium used to crosslink the matrix. There is no correlation between calcium concentration and the differentiation.

Supplementary Figure S7

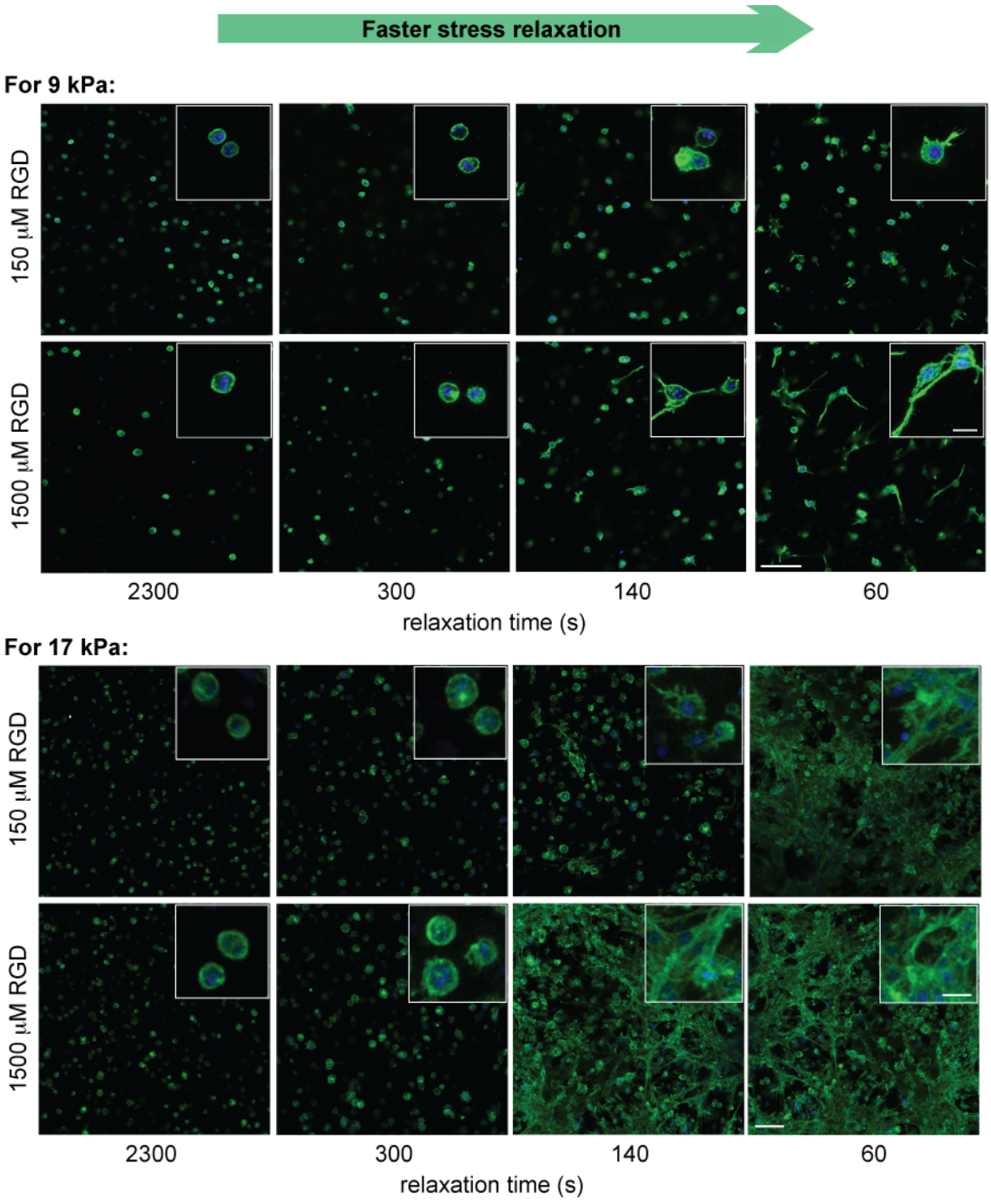

Supplementary Figure S7| MSC morphologies in gels with different initial elastic moduli, RGD ligand density, and rates of stress relaxation. Staining for actin (green) and nuclei (blue) for MSCs in

the indicated conditions. Stainings were conducted after 7 days of culture. Scale bar is 100 μm for the larger image and 20 μm for the inset.

Supplementary Figure S8

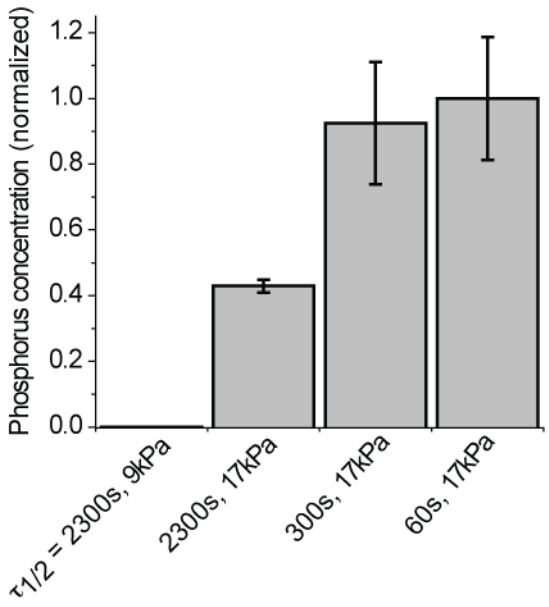

Supplementary Figure S8| Compositional analysis of alginate gels with scanning electron microscope and energy dispersive X-ray spectrometry (SEM-EDS). Phosphorus (P) concentration in cryosections of gels with the indicated conditions (all gels at 1500 μM RGD) after 2 weeks of 3D culture of MSCs. The EDS signal of P is correlated to the quantity of phosphate mineral deposit. The P signal from 9 kPa, $\tau_{1/2}$ = 2300s alginate gel (adipogenic condition) is below detection limit and not shown.

Supplementary Figure S9

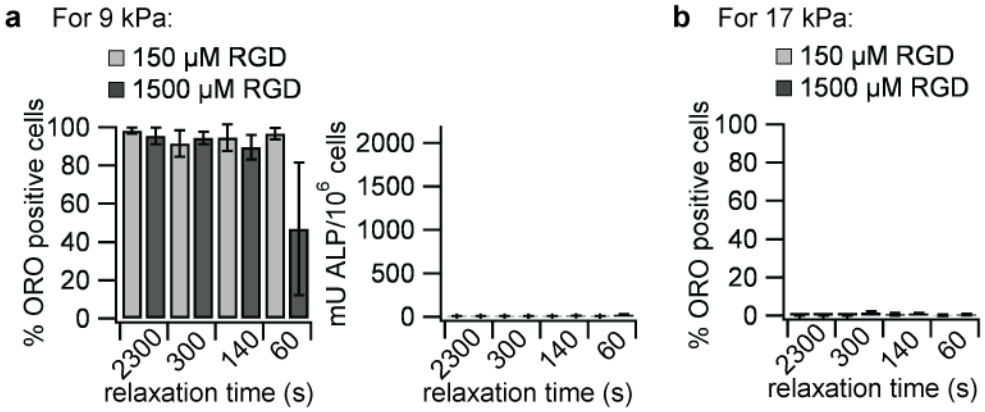

Supplementary Figure S9| Regulation of MSC differentiation by RGD ligand density. a, Quantification of percentage of cells that stain positive for ORO, and alkaline phosphatase activity for D1 cells encapsulated in gels with an initial modulus of 9 kPa and different stress relaxation timescales after 7 days in culture, at the indicated RGD ligand densities. **b,** Quantification of percentage of cells that stain positive for ORO for D1 cells encapsulated in gels with an initial modulus of 17 kPa and different stress relaxation timescales after 7 days in culture, at the indicated RGD ligand densities. The y-axis ranges in **a** and **b** are set to be equal to facilitate comparison.

Supplementary Figure S10

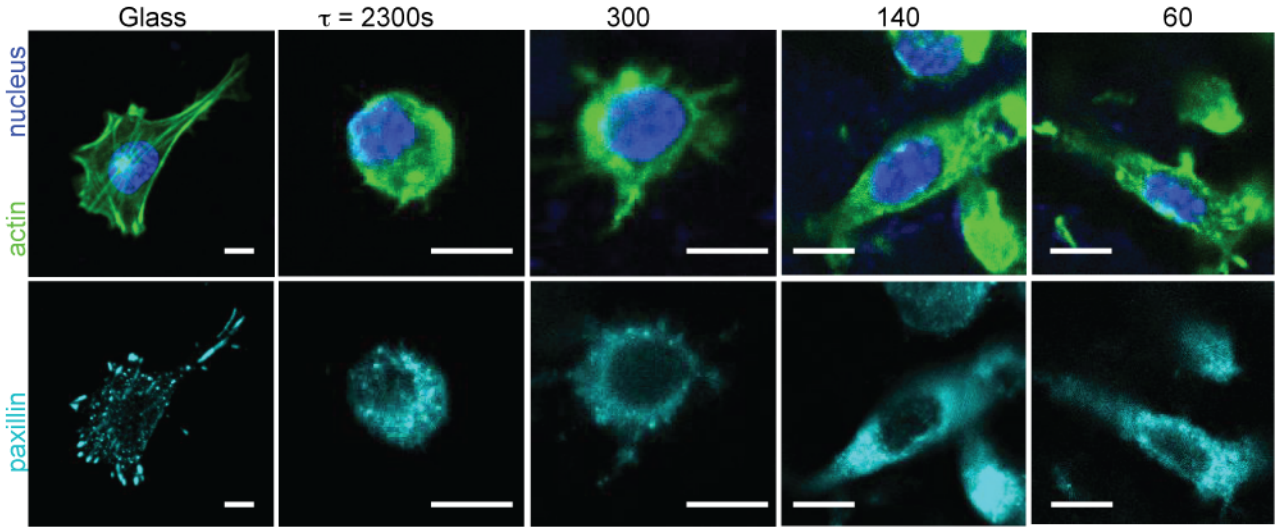

Supplementary Figure S10| No localization of paxillin to cell-ECM boundary from MSCs in alginate hydrogels is observed. Representative immunofluorescence staining for actin (green), nucleus (blue), and paxillin (cyan) in MSCs cultured on glass or within alginate hydrogels that had an initial elastic modulus of 17 kPa with the indicate timescale of relaxation. Scale bar is 10 μm.

Supplementary Figure S11

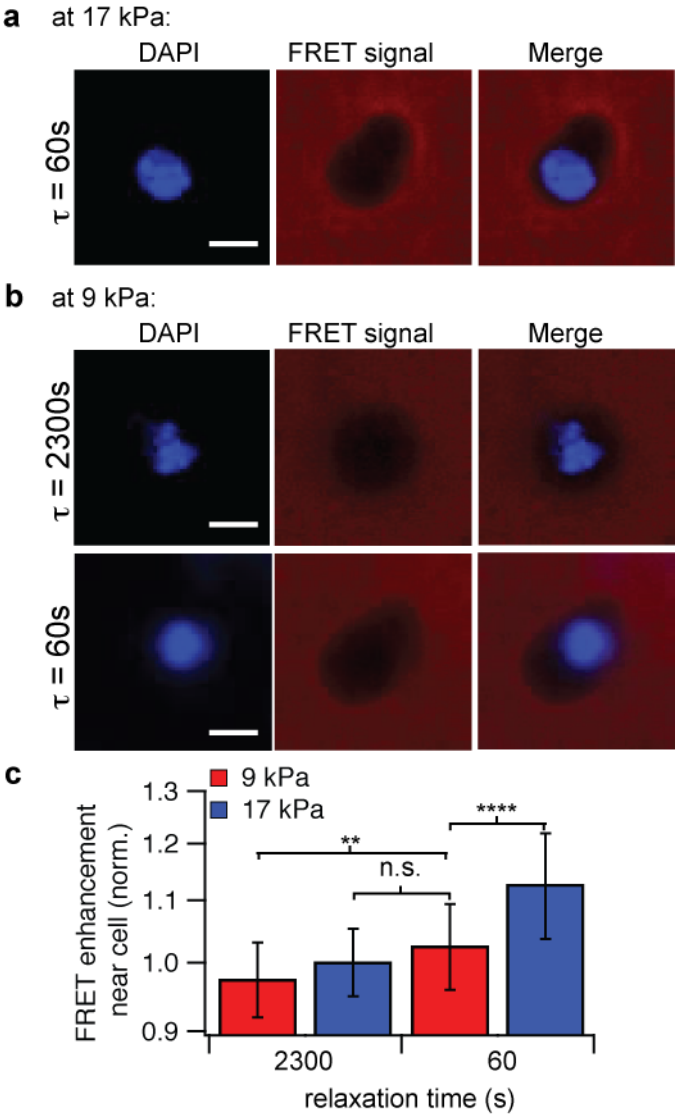

Supplementary Figure S11| RGD ligand clustering significantly lower in soft gels. a–b, Representative confocal microscope images of nucleus (DAPI/ blue) and FRET acceptor signal from hydrogel (red) surrounding MSCs cultured in hydrogels with an initial elastic modulus of 17 kPa or 9 kPa and the indicated timescales of stress relaxation after 18 hours of culture. **c,** Quantification of enhancement of FRET acceptor signal within ~2 – 3 μm of cell border relative to the background of the

hydrogel. Data are shown as mean +/- s.d. and ** indicates $p < 0.01$, **** indicates $p < 0.0001$, and n.s. indicates no statistical significance (Holm-Bonferroni test). Scale bars are all 10 μm.

Supplementary Figure S12

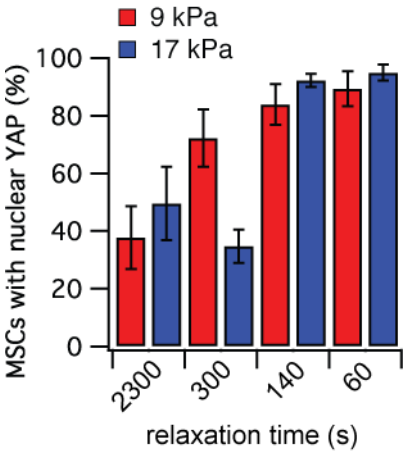

Supplementary Figure S12| Quantification of MSCs with nuclear YAP. The percentage of MSCs that exhibited nuclear YAP was quantified. Nuclear YAP increases significantly with faster stress relaxation for both initial elastic moduli (Spearman's rank correlation, $p < 0.0001$ for both).

Supplementary Figure S13

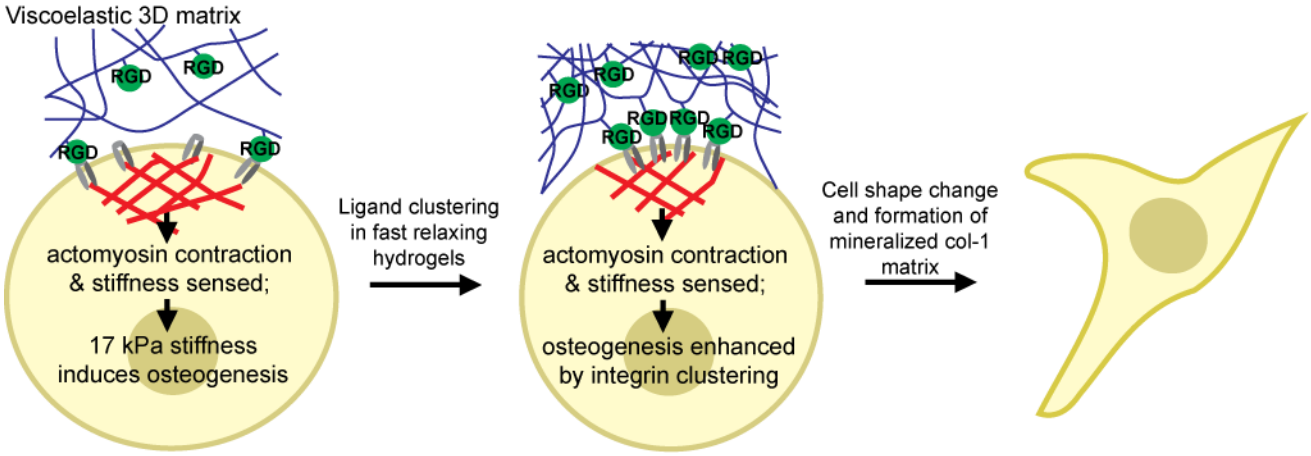

Supplementary Figure S13| Schematic of mechanism underlying MSC sensing stiffness and stress relaxation properties in viscoelastic matrices. First, MSCs bind to the viscoelastic matrix through integrins and sense matrix stiffness through actomyosin contraction. A matrix elastic modulus of 17 kPa activates osteogenic pathways. Next, ligand clustering, mediated by stress relaxation in the matrix, enhances the osteogenic signal over time. At longer timescales, the cell differentiates and is able to spread and form an interconnected and mineralized type-1 collagen rich matrix in fast relaxing gels.

Supplementary Figure S14

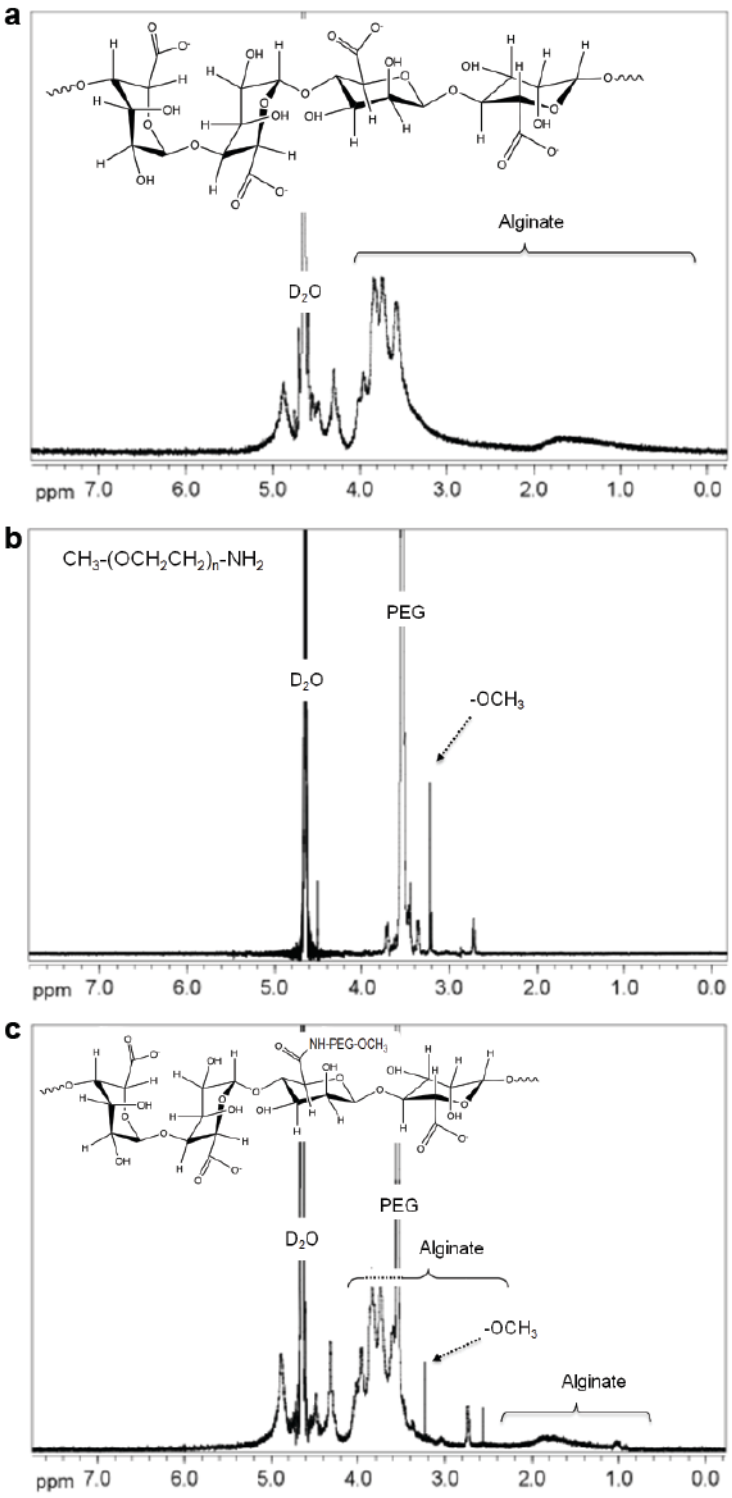

Supplementary Figure S14| ^{1}H NMR of PEG coupled alginate. ^{1}H NMR of (**a**) low MW alginate (35 kDa), (**b**) PEG-amine (5 kDa), and (**c**) PEG-alginate. Deuterated water (D_2O) was used as solvent, and

the polymer concentration was 0.5-1% (wt/vol). The efficiency of PEG engraftment was calculated based on the ratio of the integrals for alginate protons to the methyl protons from PEG's terminal methoxy group (δ ~3.2ppm). PEG-alginate was found to have approximately a PEG engraftment of 1.8 PEG per alginate backbone.

Supplementary Table 1| Peak stresses measured during stress relaxation tests of tissues

Tissue	Peak stress (Pa)
Brain (rat)	310
Liver (rat)	380
Adipose (rat)	150
Coag. Marrow (rat)	70
Fracture hematoma (human)	1,000

Supplementary Table 2| List of all hydrogel compositions used in study.

Description	MW of alginate (kDa)	cross-linker conc. (mM)	Initial elastic modulus (kPa, mean +/- s.d.)	Stress relaxation halftime, t(1/2) (s, mean +/- s.d.)
high-MW low stiffness	280	12	9.0 +/- 1.0	3300 +/- 800
mid-MW low stiffness	70	20	8.5 +/- 1.0	390 +/- 40
low-MW low stiffness	35	31	7.9 +/- 1.2	170 +/- 20
low-MW-5K PEG low stiffness	35	46	9.1 +/- 1.4	67 +/- 2
high-MW mid-stiffness	280	21	17.0 +/- 1.8	1400 +/- 60
mid-MW mid-stiffness	70	29	20.0 +/- 2.7	210 +/- 20
low-MW mid-stiffness	35	40	15.0 +/- 2.2	100+/- 20
low-MW-5K PEG mid-stiffness	35	52	15.0 +/- 1.0	44 +/- 5

Supplementary Table 3| Fit parameters for stress relaxation data

Alginate type:	280 kDa	70 kDa	35 kDa	35 kDa-5k PEG
$\tau 1$ (s)	510	125	81	39
E1 (norm.)	0.25	0.46	0.5	0.58
$\tau 2$	11111	1734	900	637
E2	0.75	0.54	0.5	0.42